

Point Cloud Representation of 3D Shape for Laser-Plasma Scanning 3D Display

Hiroyo Ishikawa and Hideo Saito
Keio University
E-mail {hiroyo, saito}@ozawa.ics.keio.ac.jp

Abstract- In this paper, a method of representing 3D shape for the laser-plasma scanning 3D display devices using point cloud in consideration of hardware is proposed. A new device has been developed for 3D spatial displays. This device generates plasma luminous bodies produced by “laser-induced breakdown” in midair. In this method, objects are represented by point cloud so that the burden of the xyz-scanner, which controls the position of the plasma, becomes lighter. Additionally, the order of drawing 3D wireframe models can be decided in consideration of the scanner burden.

I. INTRODUCTION

A new device which is able to emit plasma luminous body in midair has been developed for a new 3D display. When a high power laser beam is focused in a gas, ionization of the gas occurs. This phenomenon is called “laser-induced breakdown” and the ionized gas is “plasma”. The breakdown of air is accompanied by a bluish white light emission [1][2]. The lights produced by this device are observed as light points such as the examples in figure 1. The advantage of this device is that light points are drawn in midair without any screens. Kimura, Shimada, et al. have already developed an innovative 3D display device “Free Space Display of Point Cloud by Laser-Plasma”, that generates 3D images in midair [3]. The device is improved in order to display objects on a larger space, and various applications are considered [4].

The device continually can generate plasma luminous bodies sequentially using infrared one kilohertz pulse laser recently. The position of plasma luminous bodies can be changed by the xyz-scanner. When the distance between the plasma is short, the scanning locus seems to be expressed by a light line.

The plasma life span is very short. However, the plasma emits high intensive light. Therefore a plasma luminous body can be seen about 0.2 seconds as an afterimage, i.e. about 200 light points can be seen simultaneously. When the device scans an object at intervals of about 0.2 seconds, the still image can be observed stably.

In order to draw an object stably with these plasma light points, the number of points has to be as few as possible. However, when an object is represented with fewer points, wider gaps occur between the plasma. The xyz-scanner has to be activated quickly to scan synchronized with the plasma generation at that time; however, there is the burden of the scanner movement. The xyz-scanner cannot suddenly change

its scan direction. When data which is beyond such movement restriction is input, the light points cannot be displayed at the position that we set. Therefore, we propose a method of expression in consideration of the movement restriction of the xyz-scanner. In this method, the acceleration of the locus of the scanning becomes smooth and the change of velocity becomes slower. As the result, the plasma gap is narrow in the part of rapid change.

Furthermore, we consider the drawing method of 3D objects expressed by wireframes. When an object which is expressed with a wireframe is drawn using sequential light points, the drawing order will be a problem. When the wireframe can be expressed as an Eulerian graph, which is a graph which visits each edge exactly once, we can draw it efficiently. When the object isn't an Eulerian graph, however, some path overlaps occur. Therefore we have to choose the optimized path which is the lowest cost. We solve this problem by consideration of the length of paths and the above method which we propose.

II. DRAWING SYSTEM

The drawing system mechanism of the device is shown in figure 2. It consists of an infrared laser generator and a xyz-scanner. The laser generator continues to create one kilohertz

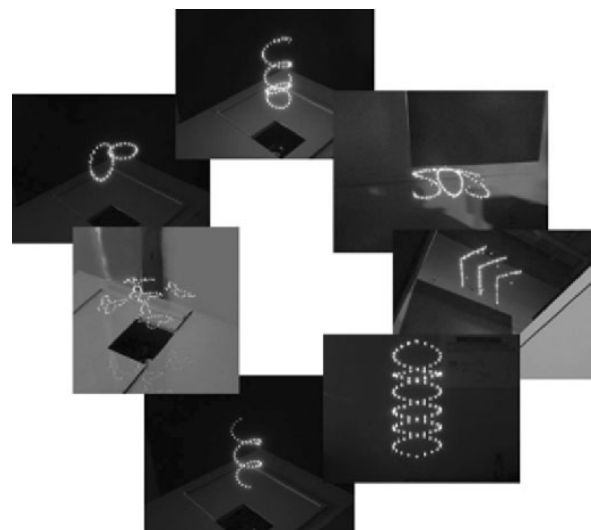


Fig. 1. Experiment scenes of the laser-plasma scanning 3D display device. These pictures are the result of the previous model of the 3D display.

pulse laser, and the xyz-scanner controls the direction of the laser beam and the distance of the focus point. The sequential plasma luminous bodies are continually generated at the arbitrary positions in midair. When the laser scans, plasma luminous bodies are drawn on the locus of the scan head.

The xyz-scanner is controlled through a D/A converter (YOKOGAWA WE7000). The WE7000 converts from the input digital data as 3D-coordinates to analog data for the xyz-scanner. The input data represents the positions of the plasma luminous bodies, and is input from a control computer, for example (0.0, 0.0, 0.0), (1.0, 0.0, 0.0). The analog data is voltage.

III. THE METHOD OF GENERATING DATA

A. Generating Points Data

An object which we try to display has to be represented as single stroke drawing. Then the positions of the plasma luminous bodies are sampled appropriately from the line. The method of sampling them is as follows.

The position of the point which is moving on the single stroke drawing is expressed with time t in (1). It is assumed that the scanner head position moves at equal speed, which is the size of the velocity and is scalar value, on the locus. The position of scanner moves a lap with a period T . The velocity, which is the vector, and the acceleration of the scanner are in (2) and (3).

$$\mathbf{r}(t) = (x(t), y(t), z(t)) \quad (1)$$

$$\mathbf{v}(t) = (v_x(t), v_y(t), v_z(t)) = \left(\frac{dx(t)}{dt}, \frac{dy(t)}{dt}, \frac{dz(t)}{dt} \right) \quad (2)$$

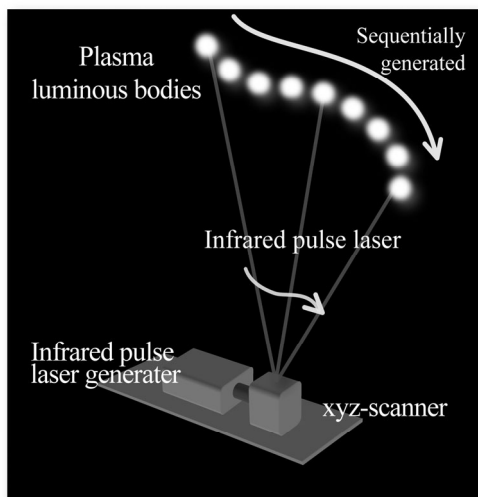


Fig. 2. The drawing system mechanism. The 3D display device consists of an infrared one kilohertz pulse laser generator and a xyz-scanner. By controlling the laser, plasmas are created at the required position. When many plasma luminous bodies are drawn fast enough (1000 point/sec).

$$\mathbf{a}(t) = (a_x(t), a_y(t), a_z(t)) = \left(\frac{dv_x(t)}{dt}, \frac{dv_y(t)}{dt}, \frac{dv_z(t)}{dt} \right) \quad (3)$$

The example of each graph in the case of a square is shown in figure 3 and 4. Here, $z(t)=0$. From these graphs, it is found that the velocity change and the acceleration are high at the corners. So the acceleration is smoothed with a simple moving average in (4). Here, the data is smoothed using neighbor data whose size is w .

$$(a_{sx}(t), a_{sy}(t), a_{sz}(t)) = \left(\frac{1}{w} \int_{t-w/2}^{t+w/2} a_x(u) du, \frac{1}{w} \int_{t-w/2}^{t+w/2} a_y(u) du, \frac{1}{w} \int_{t-w/2}^{t+w/2} a_z(u) du \right) \quad (4)$$

After the acceleration is smoothed, the velocity is calculated from the smoothed acceleration in (5). $v_{sx}(0)$, $v_{sy}(0)$ and $v_{sz}(0)$ are decide so that (6) is correct.

$$(v_{sx}(t), v_{sy}(t), v_{sz}(t)) = \left(v_{sx}(0) + \int_0^t a_{sx}(u) du, v_{sy}(0) + \int_0^t a_{sy}(u) du, v_{sz}(0) + \int_0^t a_{sz}(u) du \right) \quad (5)$$

$$\int_0^T v_{sx}(t) dt = 0, \quad \int_0^T v_{sy}(t) dt = 0, \quad \int_0^T v_{sz}(t) dt = 0 \quad (6)$$

After this process, the acceleration becomes smooth; however, the corner speed becomes slow. The original speed $V(t)$ is in (7). The smoothed speed $V_s(t)$ is in (8). They are shown in the speed graph of figure 4. It can be seen that the distance of the laser scanning becomes short from this graph,

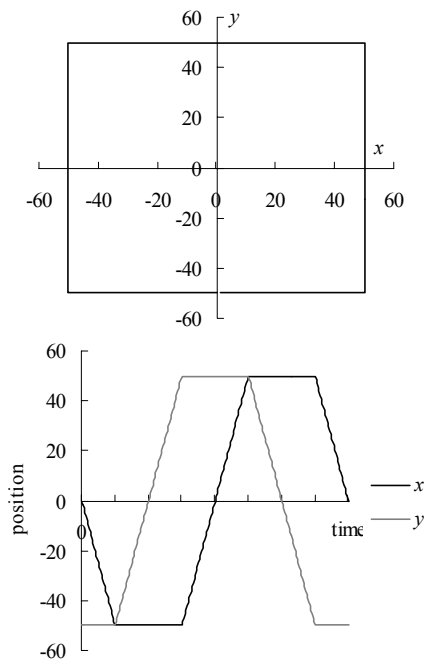


Fig. 3. Locus and position of a square. The upper graph is the locus of the scanner. The start point is (0,-50). The lower graph is the positions of x and y coordinates of the scanner.

so that the locus which is drawn using the smoothed speed becomes the square with the smoothed corners.

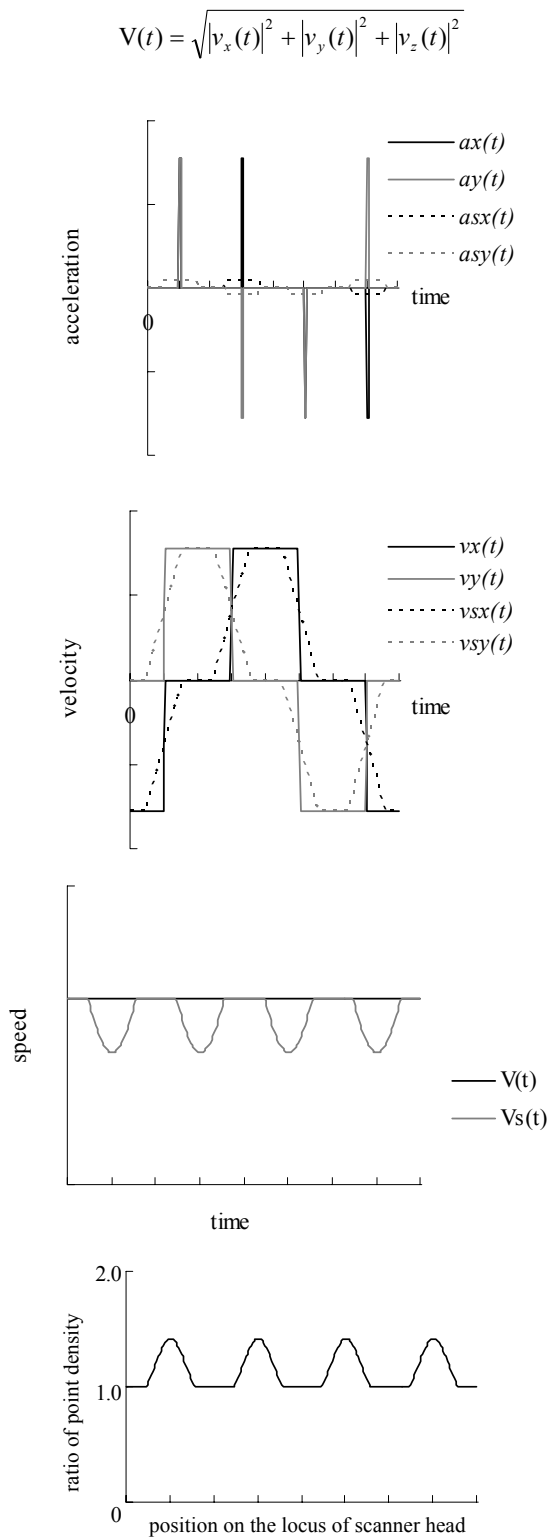


Fig. 4. Smoothing example of a square. The top graph is the velocity; the second is the acceleration of the scanner. The dotted lines are the result of smoothing ($v_{xs}, v_{ys}, a_{xs}, a_{ys}$). The third graph is the speed of the scanner. The black line is original; the gray line is the result of smoothing, the dotted line is the result of correcting. The lower graph is the point density ratio.

$$V_s(t) = \sqrt{|v_{sx}(t)|^2 + |v_{sy}(t)|^2 + |v_{sz}(t)|^2} \quad (8)$$

Therefore, it is necessary to decide the resampling positions of the plasma points based on this speed change. In the speed graph of figure 4, the point density is calculated from the ratio of $V(t)$ and $V_s(t)$, so that the integral value of $V(t)$ equals to the integral value of $V_s(t)$ at t . $V(t)/V_s(t)$ is adopted. The ratio of the point density is shown at the lower graph in figure 4. The simulation result image using this ratio of the point density is shown in figure 5. The upper image in figure 5 is the result using the same number of points (128 points) at equal intervals to compare with our method. Various 2D shapes simulation results are shown in figure 6.

B. Drawing order for wireframes

In the drawing a 3D object which is expressed by a wireframe model; it is important to decide the order of drawing paths. To solve this problem, we use a graph which is shown in figure 6. In the graph, node n_i is created from the vertices v_i of the wireframe model, and edge e_{ij} is created from the connections c_{ij} of two vertices. This is an undirected graph. An optimal route is searched, and the route is the order of drawing. The length between vertices as the cost of the edge and the angle of corner as the cost of the node are adopted as routing cost. The following way of deciding the order of drawing is applied to the graph which is created from a wireframe model.

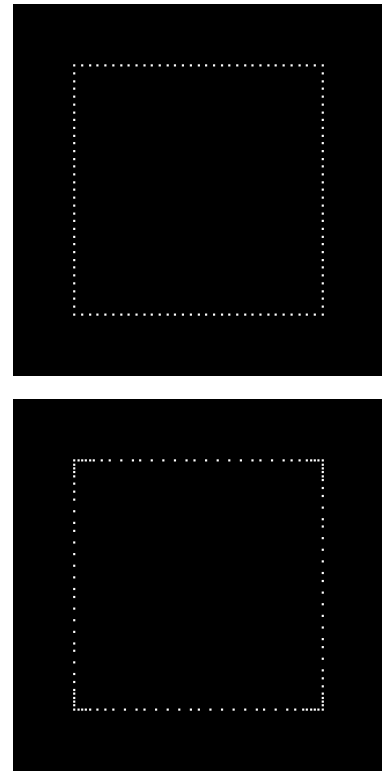


Fig. 5. The expressing result of the square. These images are display simulation results. The number of points is 128. The upper image to compare with our method is expressed at the equal intervals; the lower is expressed by our method.

1) Calculate the length of each edge.
 2) Calculate the angle formed by two edges which are input/output path of node n_i . Then calculate all the angles for all the combinations of two edges. At each node the same process is performed.

3) Search all routes which start from node n_i and pass all edges and return to n_i . If needed, it is allowable to pass an edge more than once.

4) Calculate the cost of the routes which are selected 3) by (9). The costs are two kinds, one is distance cost and the other is angle cost. Here, $L(i)$ is the i -th list of passed node. The n_1 is the start node. The n_1 and the n_{N_m} are the same node. The function $d(n_j, n_{j+1})$ is the distance between n_j and n_{j+1} . The function $angle(n_{j-1}, n_j, n_{j+1})$ is the angle which is formed by node n_{j-1} , n_j and n_{j+1} .

$$\mathbf{L}(m) = (n_1 \ \dots \ n_j \ \dots \ n_{N_m})$$

$$\text{distance_cost} = \sum_{j=1}^{N_m} d(n_j, n_{j+1})$$

$$\text{angle_cost} = - \sum_{j=1}^{N_m} angle(n_{j-1}, n_j, n_{j+1}) \quad (9)$$

5) Decide the route which has the lowest cost. The distance cost is higher priority than the angle cost. If the distance cost is the same, the angle cost is compared.

The angle cost is added to avoid the route which includes acute angles if possible. Acute angles have high cost because of using a lot of light points. Therefore, the route which includes acute angles is not selected, even if the distance cost is the same.

The result of the order deciding is shown in figure 8. The routing result is shown in table I. No. 1-4 of the result are the optimal routes. No. 5-6 are the sample routes which are the same distance cost but different angle cost.

IV. EXPERIMENTS

A. Points Data Generating Experiment

We generated the position of points data for some objects by the method which is proposed in III-A. The result of drawing a square by a real device system is shown in figure 9. The number of plasma luminous bodies is missing, however, because these photograph were taken by the camera shutter speed of 0.125 seconds. As compared with the equal intervals expression, the display for the corners of the shapes are mainly different in our method, so that the sharpness of the corners can be well represented, while there is almost no error of the position of the plasma illuminance at other parts. The results of various 2D shapes are shown in figure 10.

From these result, it is found that the burden of the scanner becomes lighter and the drawing result becomes stable. Therefore, our method is effective. Furthermore, in the case of square, the corner information is important for human perception. It can be seen that our method is effective for human perception.

B. Drawing order for wireframe experiment

We experimented to decide the drawing orders of some wireframes by the method which is proposed in III-B.

As the result, it is shown in figure 11; it is found that the route which has an acute angle is avoided from an optimal

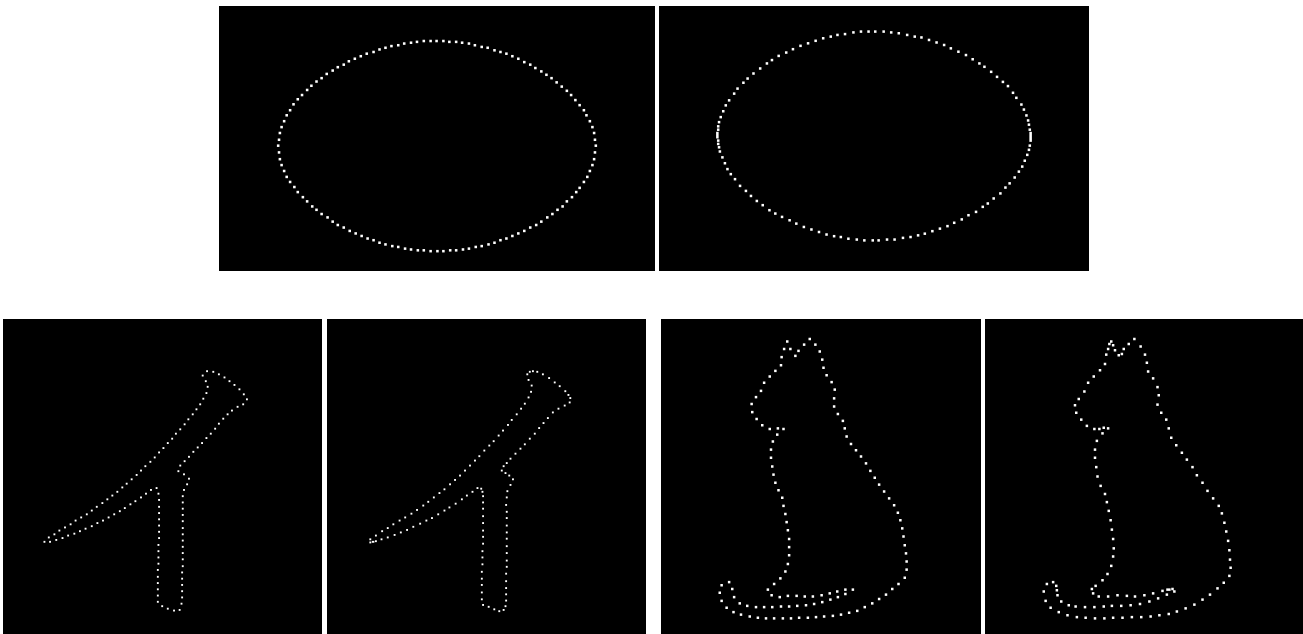


Fig. 6. The result of generating points. These images are display simulation results. The left image is created at equal intervals of points. The right image is created by our method. The number of points is 128.

route by the angle cost. Using this method, we can decide easily an optimal route.

V. CONCLUSION

We proposed a method of expressing objects in consideration of the movement restriction of the xyz-scanner of 3D spatial display device.

The effectiveness of this method was shown by the drawing experiment by the real display device system. It was found that a drawing result is stable at the same time as the burden of the scanner becomes lighter by using this method.

We experimented only for a square by the real system; however, we suppose that similar results are achieved for

other object data. In addition, we suppose that the method of deciding to the drawing order for a wire frame in consideration of the xyz scanner restriction is effective.

In this system, the object is drawn by the plasma luminous bodies which are generated sequentially, so that time lag occurs. Therefore, the number of the points that we can perceive simultaneously is limited when we try to draw a large object, and we cannot recognize the object. It can be coped by improvement of the hardware (for example, the plasma generator is increased) to solve this problem. By the improvement, it will be able to draw multi objects simultaneously, too.

ACKNOWLEDGMENT

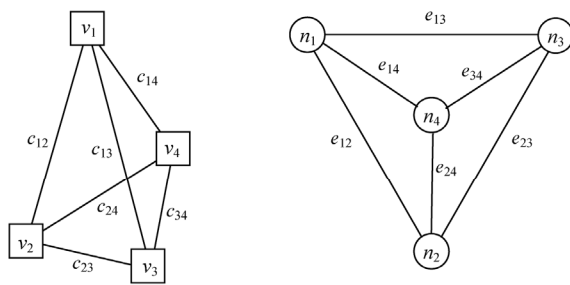
This work is supported in part by a Grant-in-Aid for the Global Center of Excellence for high-Level Global Cooperation for Leading-Edge Platform on Access Spaces from the Ministry of Education, Culture, Sport, Science, and Technology in Japan.

This work is supported in part by Core Research of Evolutional Science and Technology program (CREST) on "Technology to Display 3D Contents into Free Space" from Japan Science and Technology Agency (JST).

The authors would like to thank Mr. Hidei Kimura and Dr. Daisuke Ishikawa for of the experiments.

REFERENCES

- [1] C. De Michelis, IEEE J. Quant. Electron, QE5, pp. 188-202, 1969.
- [2] J. F. Ready, "Effects of High-power Laser Radiation" New York: Academic Press, 1971.
- [3] Kimura, H., Uchiyama, T., Yoshikawa, H., Laser produced 3D display in the air, Proceedings of Emerging technologies SIGGRAPH 2006. Boston, Massachusetts: ACM SIGGRAPH, July 2006.
- [4] H. Saito, H. Kimura, S. Shimada, T. Naemura, J. Kayahara, S. Jarusirisawad, V. Nozick, H. Ishikawa, T. Murakami, J. Aoki; A. Asano; T. Kimura, M. Kakehata, F. Sasaki, H. Yashiro, M. Mori, K. Torizuka; K. Ino, "Laser-plasma scanning 3D display for putting digital contents in free space," Proceedings of International Symposium on Electronic Imaging, Stereoscopic Displays and Applications XIX, 6803-07, California, January 2008.



v_i : i -th vertex of the wireframe model n_i : i -th node of the graph
 c_{ij} : a connection of i -th and j -th vertex e_{ij} : an edge of i -th and j -th node

Fig. 7. The example of a graph from a wireframe model. The nodes express the vertices of the wireframe, and the edges express the edges of the wireframe.

TABLE I
THE RESULT OF ROUT LIST

No.	Distance cost	Angle cost	Node list
1	1365.69	-22.63	1 2 6 7 3 2 6 5 1 4 8 7 3 4 8 5 1
2			1 2 6 7 3 4 8 5 1 4 8 7 3 2 6 5 1
3			1 4 8 5 1 2 6 7 3 4 8 7 3 2 6 5 1
4			1 4 8 7 3 2 6 7 3 4 8 5 1 2 6 5 1
5	-20.56	-20.56	1 5 8 4 3 7 6 2 1 4 8 7 3 2 6 5 1
6			1 5 8 4 1 2 6 7 3 4 8 7 3 2 6 5 1

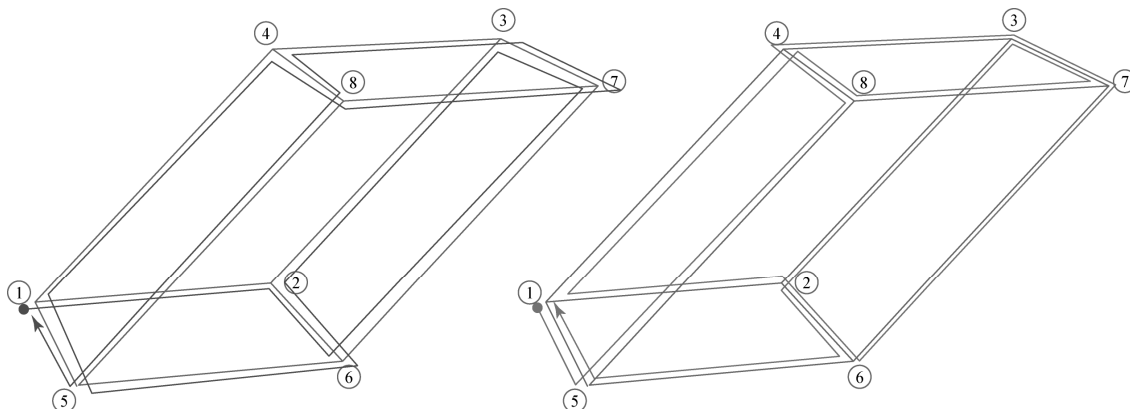


Fig.8 The result of deciding order of drawing. The left is one of the lowest cost orders, and the right is one of the orders which are not selected. They have the same distance cost, however, the angle cost is different. The dots are start node, and lines with arrow are routes.

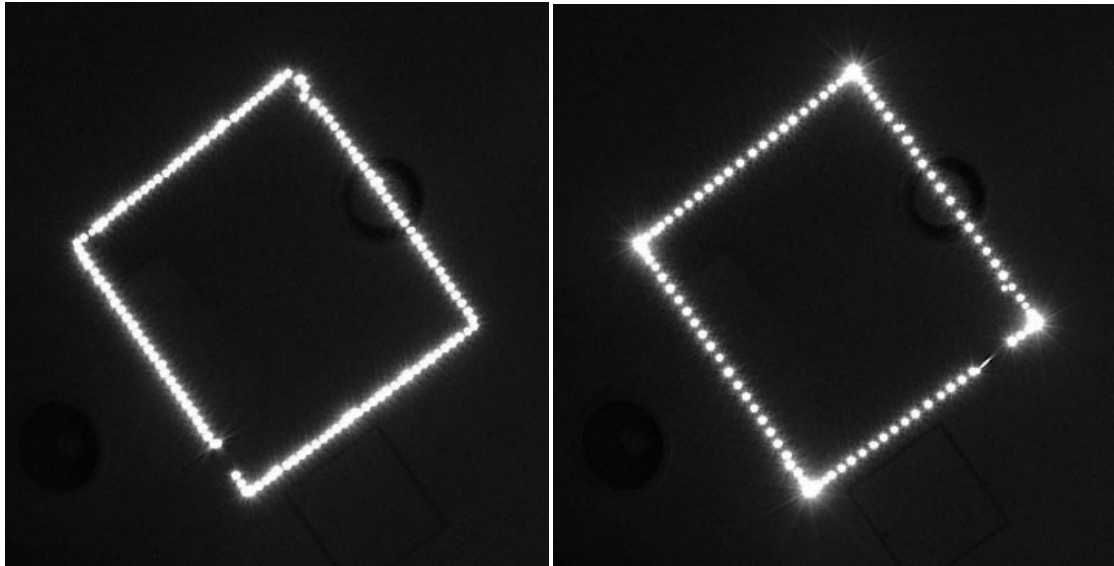


Fig. 9. The result of displaying experiments. These are real plasma luminous bodies. The left is the result of equal intervals. The right is the result of our method. These pictures were taken by the shutter speed of 0.125 seconds

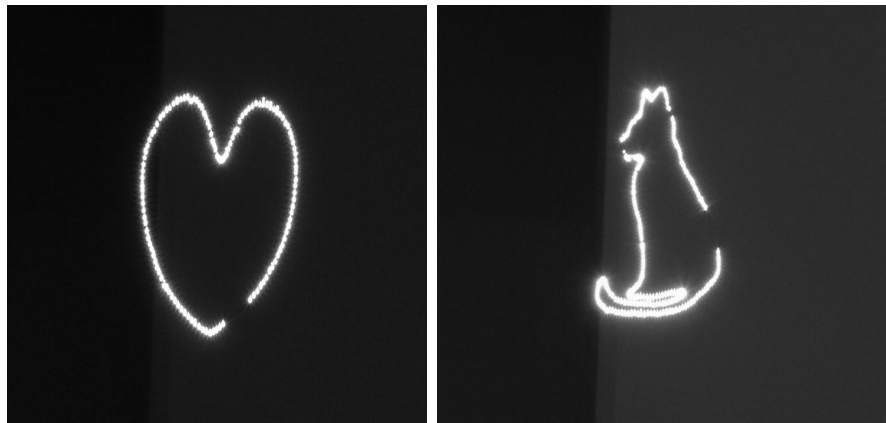


Fig.10. The result of various 2D shapes. (Shutter Speed : the left image:1/8sec, the right image 1/4sec)



Fig. 11 The result of wireframe (Shutter Speed: the left image 1/4sec,others 1/8sec)